



ELSEVIER

Polymer 44 (2003) 1681–1687

polymerwww.elsevier.com/locate/polymer

Rheological properties and interfacial tension of polypropylene–poly(styrene-*co*-acrylonitrile) blend containing compatibilizer

Y.T. Sung^a, M.S. Han^a, J.C. Hyun^a, W.N. Kim^{a,*}, H.S. Lee^b^aDepartment of Chemical and Biological Engineering, Applied Rheology Center, Korea University, Anam-dong, Seoul 136-701, South Korea^bTech. Center, LG Chemical Ltd., 84, Jang-dong, Yusung-Ku, Taejeon 305-343, South Korea

Received 10 May 2002; received in revised form 6 November 2002; accepted 2 December 2002

Abstract

Rheological and morphological properties of the polypropylene (PP) and poly(styrene-*co*-acrylonitrile) (SAN) blend containing polypropylene-*g*-poly(styrene-*co*-acrylonitrile) (PP-*g*-SAN) was studied by advanced rheometric expansion system (ARES) and scanning electron microscopy (SEM). Blends of the PP–SAN (20/80) with compatibilizer of the PP-*g*-SAN, ranging from 0 to 20 wt% (phr) were prepared using a twin screw extruder. In the study of the complex viscosity of the PP–SAN (20/80) blend, the complex viscosity of the blend showed maximum value in the 1.0 phr PP-*g*-SAN copolymer content, which suggested that the compatibilizing effect of the PP-*g*-SAN copolymer was achieved. From the morphological studies, the PP–SAN (20/80) blend showed droplet dispersion type morphology, and the PP droplet size showed minimum value (0.44 μm) in the 1.0 phr PP-*g*-SAN copolymer content. The interfacial tension of the PP–SAN (20/80) blend was determined from the morphological studies and from relaxation time using the Palierne and the Choi and Schowalter models and showed minimum value in the 1.0 phr PP-*g*-SAN copolymer content in each models. The results of the interfacial tension was consistent with the results obtained from the rheological and morphological studies of the PP–SAN (20/80) blend. From the results of the morphological, rheological studies and the values of the interfacial tension, it was suggested that the compatibility of the PP–SAN (20/80) blend increased more in the 1.0 phr PP-*g*-SAN copolymer content.

© 2003 Published by Elsevier Science Ltd.

Keywords: Polymer blend; Compatibilizer; Rheological properties

1. Introduction

Polymer blends provide an efficient way to fill new requirements for material properties [1–8]. Most polymers are immiscible from the thermodynamic point of view. As a result, immiscible blends have quite often, low mechanical properties than those of their components. It is widely known that the presence of certain polymeric species, usually suitably chosen block or graft copolymers, can alleviate to some degree of these problems as results of their interfacial activity [9–12]. The localization of the copolymer at the interface, with the block or graft extending into their respective homopolymer phases (i.e. block A in the homopolymer A phase and vice versa) not only minimizes the contacts between the unlike segments of the copolymer and homopolymer but also displaces the two homopolymers away from the interface, thereby decreasing the enthalpy of

mixing between the homopolymers [13]. Therefore, compatibility between the phases of a blend can be improved by the addition of compatibilizers which results in a finer and more stable morphology, better adhesion between the phases of the blends and consequently better properties of the final product [14]. The preferential localization of the copolymer at the interface has been shown by Brahim et al. [15], Basset et al. [16], and Hosada et al. [17] for the polyethylene (PE)–polystyrene (PS) blend, polyamide (PA)–polypropylene (PP), and maleated PP–PA blend, respectively.

A rheological study of copolymer-modified PE–PS blend by Brahim [15] showed that the dynamic viscosity at low shear rate frequencies was very sensitive to the copolymer nature and volume fraction. Germain et al. [18] reported that the rheology of PA–PP compatibilized with copolymer was highly sensitive to their initial and flow-induced morphologies. The effect of copolymer modification on linear viscoelastic properties of PS–PE blend in

* Corresponding author. Tel.: +82-2-3290-3296; fax: +82-2-926-6102.
E-mail address: kimwn@korea.ac.kr (W.N. Kim).

the molten state was investigated by Bousmina et al. [19]. In their studies, the emulsion model was used to determine the interfacial tension in unmodified and modified PS–PE blends, and 1 wt% copolymer addition to the blends resulted in a fivefold decrease of interfacial tension and particle size.

There are a few methods for the determination of the interfacial tension for the polymer blend. Among the methods, the relaxation spectrum method and morphological properties could be used for the determination of the interfacial tension between the components of blend. Using the relaxation spectrum method, Gramespacher and Meissner [21] obtained the interfacial tension of the PS–poly(methylmethacrylate) (PMMA) blend. Macaubas et al. [14], Riemann et al. [20] and Moan et al. [22] also estimated the interfacial tension of compatibilized blends like PP–PS–styrene/ethylene–butylenes/styrene triblock copolymer (SEBS), PS–PMMA–poly(styrene-*b*-methyl methacrylate) (PS-*b*-PMMA) diblock copolymer and PE–PA–maleic anhydride/acrylic ester/ethylene terpolymer, respectively.

PP and poly(styrene-*co*-acrylonitrile) (SAN) are widely used in automobile industry. Therefore, blend from them should be an ideal choice to create polymer recycling. In the present work, the influence of the graft copolymer polypropylene-*g*-poly(styrene-*co*-acrylonitrile) (PP-*g*-SAN) as a compatibilizer on the morphology and rheological properties was demonstrated. In addition, the interfacial tension of PP–SAN blend compatibilized with PP-*g*-SAN was estimated from the weighted relaxation spectrum and morphological properties. This leads to an interpretation of the compatibilized PP–SAN blend properties based on the interfacial tension and the morphological properties.

2. Experimental

2.1. Polymers

The polymers used in this study were obtained from commercial sources. The PP, used HI 520, was provided by Samsung Chemical Co. The SAN, used 81HF, was provided by LG Chemical Co. The graft copolymer PP-*g*-SAN from NOF corporation was used as compatibilizer. The melt density of the PP and SAN at 190 °C were calculated by group contribution method [23] and found to be 0.74 and 0.97 g/cm³, respectively. The characteristics and sources of the PP, SAN, and PP-*g*-SAN copolymer are shown in Table 1.

2.2. Blend preparations

Blend of PP and SAN were prepared in 20/80 weight concentration using a 42 mm diameter twin screw extruder, with a 7:1 length to diameter screw. Concentration of PP-*g*-SAN copolymer, ranging from 0 to 20 wt% (phr) with respect to the whole weight fraction of PP–SAN (20/80) blend were used.

Table 1
Characteristics of polymer samples used in the PP–SAN blend

Sample	\bar{M}_n	\bar{M}_w	MWD	Melt density (g/cm ³) ^a	T_g (°C) ^b	T_m (°C) ^b
PP ^c	4.1×10^4	2.3×10^5	5.6	0.74	–5	164
SAN ^d	5.6×10^4	1.0×10^5	1.8	0.97	107	–
PP- <i>g</i> -SAN ^e	–	–	–	–	–5, 102	160

^a Melt density at 190 °C from Ref. [23].

^b Measured in our laboratory by DSC.

^c Supplied by Samsung Chem. Co.

^d Supplied by LG Chem. Co.

^e Supplied by NOF Co. (PP–SAN = 70:30 wt%).

The polymer samples were dried under vacuum (<1 mm Hg) at 100 °C for 24 h. The temperature of the extruder was set at 160 and 190 °C in feeding and barrel zones, respectively. Samples were compression molded using a hot press at 190 °C and 40 psi for 5 min.

2.3. Scanning electron microscopy

The morphology of the cross-section of the extrudate prepared by cryogenic fracturing was examined by JEOL scanning electron microscopy (SEM) (Model JSM 5200) at 20 kV accelerating voltage after gold sputter coating (500 Å).

2.4. Rheology

Dynamic measurements were carried out on Advanced Rheometric Expansion System (ARES) in oscillatory shear at 6% strain in the parallel-plate arrangement with 25 mm plate under dry nitrogen atmosphere. The sample used in this study was fabricated in a disk with 2 mm in thickness. The frequency sweeps from 0.03 to 100 rad/s were carried out at 190 and 210 °C. The isotherm was shifted to mastercurves with a reference temperature 190 °C. For all measurement, it has been verified that the behavior of the sample was linear viscoelastic.

3. Results and discussion

3.1. Dynamic rheology

Fig. 1 shows the storage modulus (G') and loss modulus (G'') with frequency for the PP, SAN, and PP–SAN (20/80) blend at 190 °C. For the PP and SAN, the storage modulus and loss modulus shows higher for the SAN than those of the PP. For the PP–SAN (20/80) blend, the storage modulus shows higher for the either components at low frequency. At the higher frequency, the storage modulus for the PP–SAN (20/80) blend is appeared between that of the PP and SAN. This pronounced elastic properties and very long relaxation process of the immiscible polymer blends was also reported in the PS–PMMA blend [21,24] and the liquid crystalline

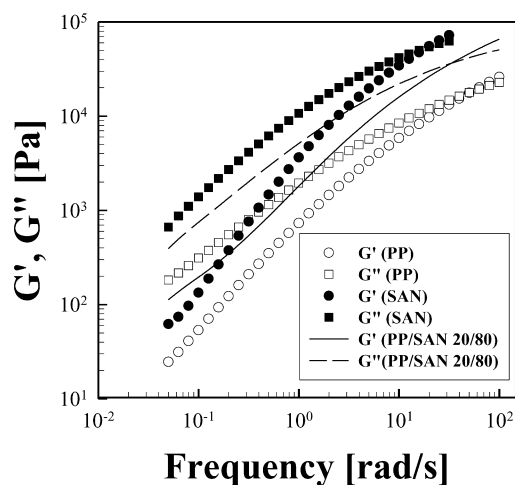


Fig. 1. Storage modulus (G') and loss modulus (G'') vs. frequency for the pure PP, SAN, and PP–SAN (20/80) blend at 190 °C. PP: (○) G' , (□) G'' ; SAN: (●) G' , (■) G'' ; PP–SAN (20/80): (—) G' , (---) G'' .

polymer with poly(ethylene terephthalate) (PET) dispersed blend [4].

Fig. 2 shows the complex viscosity of the PP–SAN (20/80) blend compatibilized with the PP-*g*-SAN copolymer. For the PP/SAN/PP-*g*-SAN (20/80/1.0) blend, the complex viscosity is increased at all the frequency compared to the PP–SAN (20/80) blend compatibilized with 5.0 and 20 phr PP-*g*-SAN copolymer. Also, the complex viscosity of the PP/SAN/PP-*g*-SAN (20/80/1.0) is increased compared to the uncompatibilized PP–SAN (20/80) blend. Table 2 shows the complex viscosity of the PP–SAN blend at 0.05 rad/s. From Table 2, the complex viscosity of the PP–SAN (20/80) blend shows maximum in the 1.0 phr PP-*g*-SAN copolymer. The increase of complex viscosity for the PP–SAN (20/80) blend compatibilized in the 1.0 phr PP-*g*-SAN copolymer may be due to the compatibilizing effect of the copolymer. When the concentration of the PP-*g*-SAN copolymer is above 1.0 phr, the separate phase of the PP-*g*-

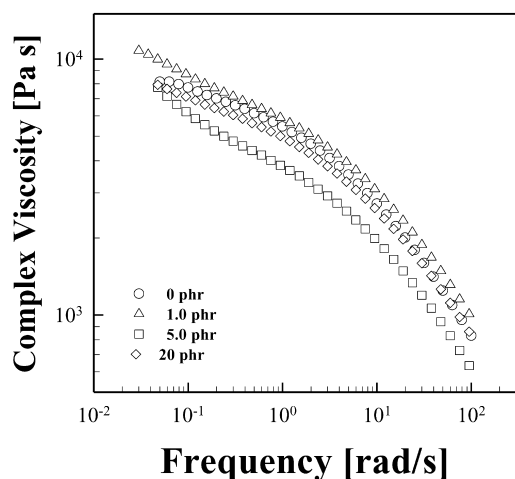


Fig. 2. Complex viscosity vs. frequency for the PP–SAN (20/80) blend compatibilized with the PP-*g*-SAN copolymer at 190 °C: (○) 0 phr; (△) 1.0 phr; (□) 5.0 phr; (◇) 20 phr.

Table 2

Complex viscosity of the PP–SAN (20/80) blend compatibilized with the PP-*g*-SAN copolymer at 0.05 rad/s

PP- <i>g</i> -SAN (phr)	Complex viscosity (Pa s)
0.0	8.2×10^3
0.3	9.2×10^3
0.5	9.3×10^3
1.0	9.6×10^3
3.0	9.3×10^3
5.0	7.2×10^3
10.0	7.4×10^3
20.0	7.7×10^3

SAN copolymer may be formed and that would cause the concentration at the low interface. Similar results was reported by Macaubas et al. [14] and Brahimi et al. [15] for the PP–PS–SBS (styrene–butylenes–styrene triblock copolymer) blend and the PE–PS–styrene–butadiene diblock copolymer blend, respectively.

Phase diagram of the PP, SAN, and PP-*g*-SAN could be obtained, however, the glass transition temperatures (T_g) of the SAN and PP-*g*-SAN were so close to each other, it was not able to detect the T_g s of the binary blends. Therefore, phase diagram of the PP, SAN, and PP-*g*-SAN could not be constructed. In our earlier studies of the poly(ether ether ketone) (PEEK)/poly(ether imide) (PEI)/polycarbonate (PC) ternary blends [11], phase diagram of the PEEK, PEI, and PC was constructed from the T_g s of the three binary blend systems.

3.2. Morphology

The morphology of the PP–SAN (20/80) blend compatibilized with the PP-*g*-SAN copolymer was studied using SEM. Fig. 3(a)–(f) shows micrographs of the cryogenically fractured cross-section surfaces for the PP–SAN (20/80) blend compatibilized with the 0, 0.3, 1.0, 5.0, 10, and 20 phr PP-*g*-SAN copolymer, respectively. From Fig. 3, the PP–SAN blend shows droplet dispersion type morphology. In Fig. 3(a)–(c), when the PP-*g*-SAN copolymer is added to the PP–SAN (20/80) blend up to 1.0 phr, the droplet size of the

Table 3

Number average radius (R_i) and volume average radius (R_v) of the PP–SAN (20/80) blend as function of the concentration of the PP-*g*-SAN

PP- <i>g</i> -SAN (phr)	R_i (μm) ^a	R_v (μm) ^a
0	1.01	1.21
0.3	0.57	0.68
0.5	0.55	0.66
1.0	0.44	0.53
3.0	0.60	0.72
5.0	0.58	0.70
10	0.54–1.96	–
20	0.54–3.13	–

^a R_i and R_v were determined using image analyzer.

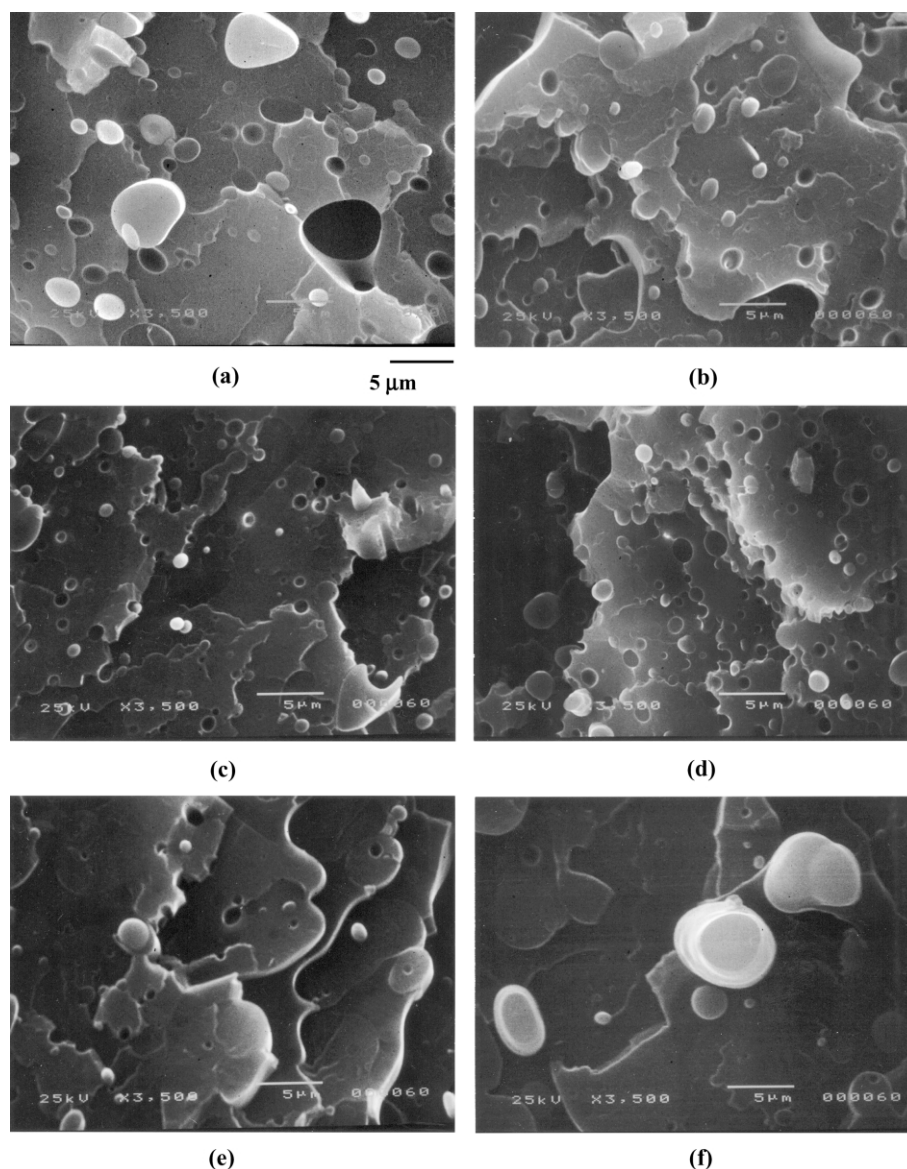


Fig. 3. SEMs obtained from cryogenically fractured cross-section surfaces of the PP–SAN (20/80) blend compatibilized with the PP-*g*-SAN copolymer: (a) 0 phr; (b) 0.3 phr; (c) 1.0 phr; (d) 5.0 phr; (e) 10 phr; (f) 20 phr.

PP is decreased from 1.01 to 0.44 μm with the increase of weight fraction of the PP-*g*-SAN copolymer (Table 3). When the PP-*g*-SAN copolymer concentration is higher than 1.0 phr, it is observed that the droplet size of the PP is increased from 0.44 to 3.13 μm . From Table 3 and Fig. 3, it is shown that the droplet size of the PP is minimum (0.44 μm) in the PP/SAN/PP-*g*-SAN (20/80/1.0) blend, which suggests the increase of the compatibility between the PP and SAN. This result is consistent with the result obtained from the dynamic rheology of the PP–SAN (20/80) blend, which is the complex viscosity of the PP/SAN/PP-*g*-SAN blend shows maximum in the 1.0 phr PP-*g*-SAN copolymer due to the compatibilization effect of the PP-*g*-SAN copolymer.

3.3. Interfacial tension of PP and SAN

Fig. 4 shows the weighted relaxation spectrum ($\tau H(\tau)$) with the relaxation time (τ) for the PP and SAN. The weighted relaxation spectrum was obtained from the storage modulus data is shown in Fig. 1. To get the weighted relaxation spectrum ($\tau H(\tau)$) of the PP and SAN, Eqs. (1) and (2) are introduced, which is related to the experimental value of G' and G'' [25]:

$$G'(\omega) = \int_{-\infty}^{\infty} [H(\tau)\omega^2\tau^2/(1 + \omega^2\tau^2)]d(\ln \tau) \quad (1)$$

$$G''(\omega) = \int_{-\infty}^{\infty} [H(\tau)\omega\tau/(1 + \omega^2\tau^2)]d(\ln \tau) \quad (2)$$

The relaxation spectrum ($H(\tau)$) can be determined using the

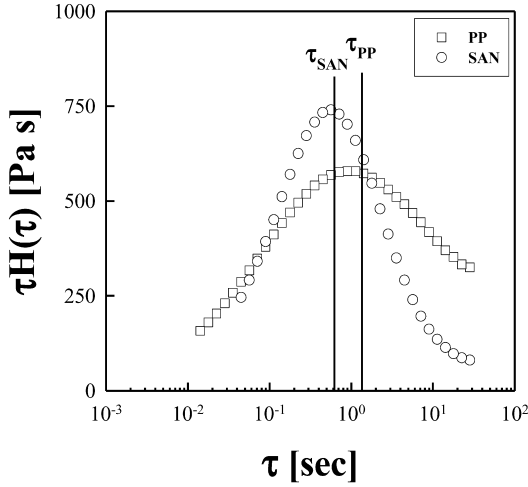


Fig. 4. Weighted relaxation spectrum of the PP and SAN: (□) PP; (○) SAN.

Tschoegle approximation [26] as shown in Eq. (3):

$$H(\tau) = G' [d \log G' / d \log \omega - \frac{1}{2} (d \log G' / d \log \omega)^2 - (1/4.606) d^2 \log G' / d (\log \omega)^2]_{1/\omega = \tau/\sqrt{2}} \quad (3)$$

where ω is the frequency and τ is the relaxation time. From Fig. 4, it is observed that the relaxation time of the PP and SAN is found at about 1.2 and 0.6 s, respectively.

Fig. 5 shows the weighted relaxation spectrum of the PP–SAN (20/80) blend compatibilized with 0, 0.3, 0.5, 1.0, and 3.0 phr PP-g-SAN copolymer. For the uncompatibilized PP–SAN (20/80) blend in Fig. 5, two relaxation spectrum peaks are observed at about 0.7 and 14.2 s, respectively. The first peak (0.7 s) is related to the phases of the components (PP and SAN) and the second peak (14.2 s) corresponding to the long relaxation time is associated with the contribution

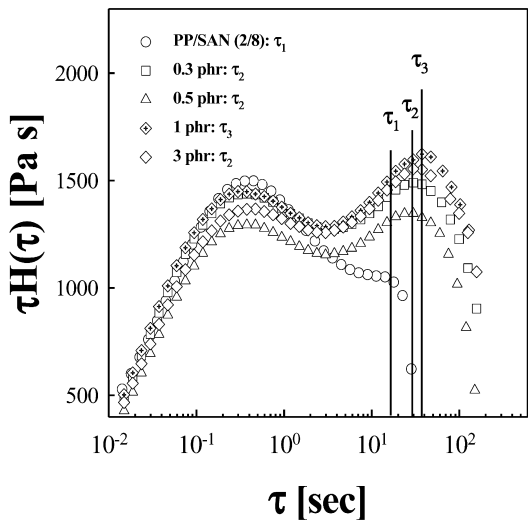


Fig. 5. Weighted relaxation spectrum of the PP–SAN (20/80) blend with the PP-g-SAN copolymer concentration: (○) 0 phr; (□) 0.3 phr; (△) 0.5 phr; (◇) 1.0 phr; (◇) 3.0 phr.

of the interphase of the PP and SAN blend [14,20–22]. As shown in Fig. 4, relaxation times of the PP and SAN were so close that the relaxation of the PP and SAN was superimposed in the first peak of the Fig. 5. In Fig. 5, when the PP-g-SAN copolymer is added to the PP–SAN (20/80) blend up to 1.0 phr, the second relaxation time is increased from 14.2 to 37.4 s (Table 4). Similar result was reported by the Macaubas et al. [14] for the PP–PS-styrene/ethylene–butylenes/styrene triblock copolymer (SEBS) blend where the form relaxation time showed maximum value with the compatibilizer content. When the PP–SAN (20/80) blend compatibilized with 3.0 phr PP-g-SAN copolymer, the second relaxation time is decreased from 37.4 to 29.7 s (Table 4).

Fig. 6 shows the weighted relaxation spectrum of the PP–SAN (20/80) blend compatibilized with 5.0, 10, and 20 phr PP-g-SAN copolymer. When the PP-g-SAN copolymer is added 5.0 and 10 phr, it is observed that the second relaxation time is decreased from 37.4 to 14.9 s (Table 4). For the PP–SAN (20/80) blend compatibilized with 20 phr PP-g-SAN copolymer, the second relaxation time is not able to detect since the PP-g-SAN copolymer is segregated as the third phase. Similar results was observed by Macaubas et al. [14] for the PP–PS–SBS (styrene–butylenes–styrene triblock copolymer) blend.

To get the interfacial tension of the PP–SAN (20/80) blend, we used Palierne emulsion model [27] shown in Eq. (4). The form relaxation time (τ_1) corresponding to the second relaxation time shown in Figs. 5 and 6 is expressed in Eq. (4):

$$\tau_1 = \frac{R_v \eta_m (19K + 16)(2K + 3 - 2\phi(K - 1))}{4\alpha (10(K + 1) - 2\phi(5K + 2))} \quad (4)$$

where τ_1 is the form relaxation time due to the relaxation of the interface, η_m is the viscosity of the matrix, α is the interfacial tension of the blend, ϕ is the volume fraction of the dispersed phase, and $K = \eta_i/\eta_m$ is the zero shear viscosity ratio of the droplet and matrix.

Interfacial tension was also obtained from Choi–Schowalter model shown in Eq. (5) [28]. The form relaxation time (τ_1) and the interfacial tension (α) is related

Table 4
Form relaxation time (τ_1) and interfacial tension (α) for the PP–SAN (20/80) blend compatibilized with the PP-g-SAN copolymer

PP-g-SAN (phr)	τ_1 (s)	α_1^a (mN/m)	α_2^b (mN/m)
0	14.2	2.13	3.50
0.3	29.7	0.57	0.94
0.5	29.7	0.56	0.92
1.0	37.4	0.35	0.56
3.0	29.7	0.62	0.91
5.0	14.9	1.15	1.72
10	14.9	–	–
20	–	–	–

^a α_1 was calculated from the Palierne emulsion model [27].

^b α_2 was calculated from the Choi–Schowalter emulsion model [28].

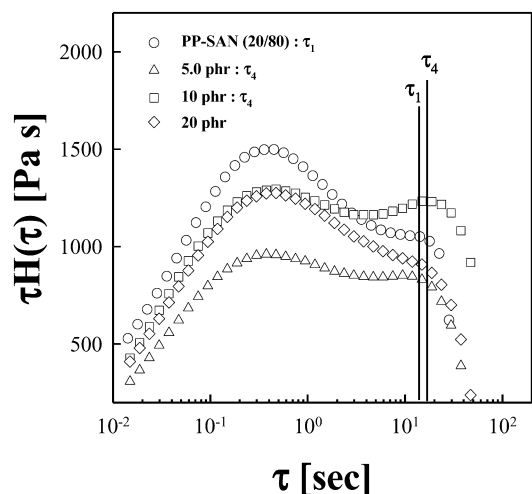


Fig. 6. Weighted relaxation spectrum of the PP–SAN (20/80) blend with the PP-*g*-SAN copolymer concentration: (○) 0 phr; (△) 5.0 phr; (□) 10 phr; (◇) 20 phr.

as follows:

$$\tau_1 = \frac{R_v \eta_m}{\alpha} \frac{(19K + 16)(2K + 3)}{40(K + 1)} \times \left[1 + \phi \frac{5(19K + 16)}{4(K + 1)(2K + 3)} \right] \quad (5)$$

Applying Eqs. (4) and (5) to the PP–SAN (20/80) blend, the interfacial tension of the PP–SAN (20/80) blend can be obtained in each model.

Table 4 shows the interfacial tension of the PP–SAN (20/80) blend calculated from the Palierne and the Choi–Schowalter models. From the Palierne model, the interfacial tension of the PP–SAN (20/80) blend shows minimum value (0.35 mN/m) in the 1.0 phr PP-*g*-SAN copolymer content, which suggests that compatibility is increased at this copolymer content. For the Choi and Schowalter model, the interfacial tension shows also minimum value (0.56 mN/m) in the 1.0 phr PP-*g*-SAN copolymer content, which represents similar trend with the result obtained by Palierne model. The results of the interfacial tension (α) and form relaxation time (τ_1) are consistent with the results obtained from the morphological and complex viscosity studies of the PP–SAN (20/80) blend. From the above results of the morphological and rheological studies and the interfacial tension data shown in Tables 2–4, it is suggested that compatibility of the PP–SAN (20/80) blend is increased more in the 1.0 phr PP-*g*-SAN copolymer content.

4. Conclusions

In this study, morphological and rheological properties of the PP–SAN (20/80) blend compatibilized with the PP-*g*-SAN copolymer were investigated. In the study of the effect of compatibilizer on the rheological properties of the PP–SAN (20/80) blend, the complex viscosity of the PP–SAN

(20/80) blend was increased in the 1.0 phr PP-*g*-SAN copolymer content. The increase of the complex viscosity of the PP/SAN/PP-*g*-SAN (20/80/1.0) blend suggests that the compatibility is increased in the 1.0 phr PP-*g*-SAN copolymer content.

In the study of morphology by SEM for the PP–SAN (20/80) blend, the continuous phase and dispersed phase were observed. At the 1.0 phr PP-*g*-SAN copolymer content, the droplet size of the PP showed minimum value (0.44 μm) in the PP–SAN (20/80) blend. From the above results of the complex viscosity and morphological study, it can be concluded that the compatibility is increased for the PP/SAN/PP-*g*-SAN (20/80/1.0) blend.

From the weighted relaxation spectrum of the PP–SAN (20/80) with compatibilizer, we have determined the interfacial tension of the blend. The interfacial tension of the PP–SAN (20/80) blend was calculated using the Palierne and the Choi and Schowalter models and showed minimum value in the 1.0 phr PP-*g*-SAN copolymer content. The results of interfacial tension are consistent with the results obtained from the rheological and morphological studies of the PP–SAN (20/80) blend.

From the above results of the morphological, rheological studies and the values of the interfacial tension, it can be concluded that the compatibility of the PP–SAN (20/80) blend increases more in the 1.0 phr PP-*g*-SAN copolymer content.

Acknowledgements

This study was supported by research grants from the Korea Science and Engineering Foundation (KOSEF) through the Applied Rheology Center (ARC), an official KOSEF-created engineering research center (ERC) at Korea University, Seoul, Korea.

References

- [1] Sundaraj U, Macosko CW. *Macromolecules* 1995;28:2647.
- [2] Han MS, Giles DW, Kim WN. *Polym Engng Sci* 2001;41:1506.
- [3] Han MS, Park JH, Cheen SW, Kim SH, Kim WN. *Polym Bull* 2000; 45:151.
- [4] Kim WN, Denn MM. *J Rheol* 1992;36:1477.
- [5] Lee HS, Denn MM. *J Rheol* 1999;43:1583.
- [6] Lee HS, Denn MM. *Kor–Aust Rheol J* 1999;11:266.
- [7] Chun YS, Han MS, Park JH, Kim WN. *Kor–Aust Rheol J* 2000;12: 101.
- [8] Choi JH, Ryu JH, Kim SY. *Kor–Aust Rheol J* 2000;12:135.
- [9] Anastasiadis SH, Gancarz I, Koberstein JT. *Macromolecules* 1989;22: 1449.
- [10] Han MS, Lim BH, Jung HC, Hyun JC, Kim WN, Kim SR. *Kor–Aust Rheol J* 2001;13:169.
- [11] Chun YS, Kwon HS, Kim WN, Yoon HG. *J Appl Polym Sci* 2000;78: 2488.
- [12] Kim JH, Kim MJ, Kim CK, Lee JW. *Kor–Aust Rheol J* 2001;13:125.
- [13] Wenchun H, Koberstein JT, Lingelser JP, Gallot Y. *Macromolecules* 1995;28:5209.

- [14] Macaubas PHP, Demarquette NR. *Polymer* 2001;42:2543.
- [15] Brahim B, Ait-Kadi A, Aji A, Jerome R, Fayt R. *J Rheol* 1991;35:1069.
- [16] Basset D, Lecerf F, Martin JM. *Colloque Francais-Iberique de Microscopie Electronique*. 1991, July.
- [17] Hosada S, Kojima K, Kanda Y, Aoyagi M. *Polym Networks Blends* 1991;1:51.
- [18] Germain Y, Ernst B, Genelot O, Dhamani L. *J Rheol* 1994;38:681.
- [19] Bousmina M, Bataille P, Sapiha S, Schreiber HP. *J Rheol* 1995;39:499.
- [20] Riemann RE, Cantow HJ, Friedrich Chr. *Macromolecules* 1997;30:5476.
- [21] Gramespacher H, Meissner J. *J Rheol* 1992;36:1127.
- [22] Moan M, Huitric J, Mederic P, Jarrin J. *J Rheol* 2000;44:1227.
- [23] Van Krevelen DW. *Properties of polymers*. New York: Elsevier; 1990.
- [24] Graebling D, Muller R, Paliarne JF. *Macromolecules* 1993;26:320.
- [25] Ferry JD. *Viscoelastic properties of polymers*. New York: Wiley; 1980.
- [26] Tschoegl NW. *The phenomenological theory of linear viscoelastic behavior*. Berlin: Springer; 1989.
- [27] Paliarne JF. *Rheol Acta* 1990;29:204.
- [28] Choi SJ, Schowalter WR. *Phys Fluids* 1975;18:420.